

.....

# **NANOMATERIALS IN CONCRETE**

.....

**Advances in Protection,  
Repair, and Upgrade**

**Henry E. Cardenas, Ph.D.**

*Associate Professor of Mechanical  
and Nanosystems Engineering  
Louisiana Tech University*



**DEStech Publications, Inc.**

## **Nanomaterials in Concrete**

DEStech Publications, Inc.  
439 North Duke Street  
Lancaster, Pennsylvania 17602 U.S.A.

Copyright © 2012 by DEStech Publications, Inc.  
All rights reserved

No part of this publication may be reproduced, stored in a retrieval system, or transmitted, in any form or by any means, electronic, mechanical, photocopying, recording, or otherwise, without the prior written permission of the publisher.

Printed in the United States of America  
10 9 8 7 6 5 4 3 2 1

Main entry under title:  
Nanomaterials in Concrete: Advances in Protection, Repair, and Upgrade

A DEStech Publications book  
Bibliography: p.  
Includes index p. 171

ISBN: 978-1-60595-050-1

*To  
Tracy, Matthew, Bethany, and Robbie*



# Table of Contents

*Acknowledgements* xi

*Introduction* xiii

<b>1. Nanomaterial Application Methods</b> .....	<b>1</b>
1.1. Doping	1
1.2. Electrodeposition Coagulation Assembly	3
1.3. Electrostatic Assembly	5
1.4. Sintering	5
1.5. Reactive Conversion	6
1.6. Pore Assembly	6
<b>2. Permeability Reduction</b> .....	<b>9</b>
2.1. Permeability and the Wet Basement	9
2.2. Radical Permeability Reduction	24
2.3. References	27
<b>3. Porosity Reduction and Strength Increase</b> .....	<b>29</b>
3.1. Porosity Reduction	29
3.2. Strength Enhancement	35
3.3. References	39

<b>4. Crack Repair</b> .....	<b>41</b>
4.1. Getting Nanoparticles to a Crack Repair	42
4.2. Simulating the Particle Packing Process for Crack Repair	44
4.3. Placing the Particle Packing Electrode	47
4.4. Optimizing the Packing Electrode Placement	48
4.5. Summary of Electrokinetic Crack Repair	53
4.6. References	53
<b>5. Chloride Extraction and Nanoparticle Barrier Formation</b> .....	<b>55</b>
5.1. Chlorides and Corrosion	55
5.2. Chloride Removal from Structures	56
5.3. Adding Nanoparticles to the ECE Process	57
5.4. Nanoparticle Packing and Corrosion Performance	60
5.5. Nanoparticles and the Chloride Barrier	61
5.6. Pore Volume and Structure Revisions	62
5.7. Microstructural Phases Generated by Nanoparticles	64
5.8. Summary of Nanoparticle Assisted Corrosion Mitigation	70
5.9. References	70
<b>6. Sulfate Removal and Damage Recovery</b> .....	<b>73</b>
6.1. Sulfate Attack Prevention	73
6.2. Using Nanoparticles to Address Sulfate Attack	74
6.3. Assessing Sulfate Damage	76
6.4. Treatment Impact on Sulfate Attack	78
6.5. Summary of Sulfate Decontamination and Recovery	84
6.6. References	85
<b>7. Freezing-Thaw Damage Reversal</b> .....	<b>87</b>
7.1. Freeze-Thaw and the Disappointment of Sealants	87
7.2. Getting Nanoparticles into Vertical Façade Structures	88
7.3. A New Freeze-Thaw Resistant Nanocomposite	90
7.4. Great Composite Strength Enhancement	92
7.5. Cracks vs. Pores	94
7.6. The Damage Recovery Treatment	96
7.7. The Preventative Treatment	96

7.8. Summary of Treatment for Freezing and Thawing Resistance	96
7.9. References	97
<b>8. Electrokinetic Nanomaterial Process Control and Design</b>	<b>99</b>
8.1. Transport Control	99
8.2. Transport Phenomena in Concrete	101
8.3. Electrokinetic Transport	105
8.4. Nanoparticle Transport Modeling in Concrete	113
8.5. Calculating Transport Rates and Particle Dosages	120
8.6. Particle Size and Dosage Levels	121
8.7. Establishing and Maintaining Particle Delivery Circuits	124
8.8. Example Nanoparticle Treatment Design: Concrete Bridge Deck	142
8.9. References	146
<b>9. Electromutagenics</b>	<b>149</b>
9.1. Pore Structure Revision	149
9.2. Chemical Activation/Microstructural Phase Revision	151
9.3. Polymeric Phase Assembly	154
9.4. Nanocomposite Phase Assembly	158
9.5. Lithium-Coated Silica Treatment	166
9.6. Opportunities	168
9.7. References	169
<i>Index</i>	171
<i>About the Author</i>	177





# Acknowledgements

I wish to express my gratitude to Dr. Leslie Struble, Professor of Civil Engineering, University of Illinois Urbana-Champaign (UIUC), for her advice and support, and for graciously making her time, laboratory, and information resources extensively available at the beginning of this odyssey. The generous insight of Dr. Thomas Mason, Professor of Material Science, Northwestern University in Evanston, Illinois, is especially appreciated.

Deep gratitude is expressed to the author's late father, Victor M. Cardenas, Chemical Engineer, Vanex Color of PPG Industries, Mt. Vernon, Illinois. His inspiration and extensive technical assistance in the laboratory was phenomenal. I wish he could be here to see this project completed.

The author also wishes to extend his sincere appreciation to Mr. David Hodge, President of Litania Sports, in Urbana, Illinois for the initial financial and moral support of this work. Other generous sponsors include Ron Smith, HRS LLC, Paul Femmer, Osmotec, LLC, Dr. Paul Todd, TechShot Inc., Charles Turk, Entergy Nuclear, Inc., U.S. Army Corps of Engineers, NASA Kennedy Space Center, and the A. J. Weller Corporation. Significant material and technical support that was much appreciated, was also provided by John Grim and John Hughes, Applications Engineers with Nalco Chemical. Thanks are also extended to the technical sales staff at Oxychem for provision of other test materials. Mr. Bryant Mather, past president of the American Concrete Institute and the American Society of Materials and Testing is gratefully acknowledged for his generous insight and technical information, as is also Dr. Francis Young, Professor Emeritus of Civil Engineering at UIUC, for his sage experimental advice.

The efforts of several of my past students have also contributed greatly to this project. I wish to thank Dr. Kunal Kupwade-Patil for his relentless effort, support, and enormous productivity. My sincere appreciation also goes to Aliya Arenova, Anupam Joshi, Dr. James Philips, Josh Alexander, Anjaneyulu Kurukunda, Mark Castay, James Eastwood, Syed Faisal, Nagaraju Goli, Padmanabhan Venkatachalam, Shailesh Madiseti, Oner Moral, Johnathan Needham, Israel Popoola, Lakshim Rachapudi, Shailesh Madiseti, Pradeep Paturi, Ralph Serrano, Nicholas Richardson, and Joey Zhao.

My multi-disciplinary collaborators from Louisiana Tech University have had a tremendous impact on making many of the findings in this work possible. Dr. Jinko Kanno, Mathematics, Dr. Daniela Mainardi, Chemistry, Dr. Sven Eklund, Chemistry, Dr. Sidney Sit, Biomedical Engineering, Dr. Yuri Lvov, Physics, and Dr. Luke Lee, Civil Engineering have all blessed this work with valuable contributions. From Kennedy Space Center, the Corrosion Technology Group, Dr. Luz Marina Calle, Dr. Mark Kolody, Dr. Paul Hintze, Dr. Wendy Li, Mr. Joe Curren are also deeply appreciated.

Above all, I wish to thank my wife, Tracy Cardenas, for her gracious support, understanding, and sacrifice; and my children, Matthew, Bethany, and Robbie, for their patience and inspiration.

# Introduction

**I**T is widely noted that advances in nanotechnology will have a disruptive impact on society. Nanosystems engineering is expected to change the way we live as much as the train, the automobile, or the computer. It is remarkable that during our 5000 year history with concrete we have gone about our lives giving little thought to the surfaces and structures upon which we work, live and drive. In contrast, today's era of rapid global economic development is straining our capacity to build and sustain the infrastructure of civilization, because modern concrete manufacturing leaves an ecological footprint second only to the combustion engine. At the same time, the need to construct concrete that is strong and durable has never been greater—an imperative surpassed only by the need to sustain the durability of existing structures instead of rebuilding them. This text describes recent advances in nanomaterials processing which offer historic opportunities for minimizing the financial and ecological burdens required to maintain these essential assets.

Until now, concrete structural enhancement could only be engaged at the point of construction, while the mix is being formed. For concrete rehabilitation, repairs could only be achieved by adding on to the structure, and this often requiring partial demolition. Recent developments in nanotechnology are starting to change the rules. The fertile combination of electrokinetic processing and nanoparticle engineering has opened the door to a broad spectrum of alternative repair strategies ranging from decontamination, permeability reduction, and strength enhancement, to remediation from various types of chemical degradation processes. Remarkable structural repairs and upgrades are now possible

using nanomaterials and electromutagenic processing methods that can radically reconfigure the microstructure of common building materials and provide significant service life extensions without changing the physical dimensions or the external appearance of the structure.

The book is written to address the interests of the researcher and the engineer. Chapter 1 introduces the ways in which nanomaterials are applied. Much of this section focuses on specific phase development and modification methods as influenced by particle selection and electric field application. Chapters 2 through 4 focus on the basic applications of nanomaterial modifications to concrete. These include permeability reduction, porosity reduction, strength enhancement, and crack repair. More specialized durability applications are explored in Chapters 5 through 7. These include mitigation of reinforcement corrosion, recovery from sulfate attack, and recovery from freeze-thaw damage. Chapter 8 presents the practical engineering aspects of planning, setting up, and executing a given treatment application. In Chapter 9 the concept of electromutagenic processing is introduced, and specific opportunities are described for radical changes to both concrete microstructures and the properties that depend upon them. This book represents a small step in the early progress of a growing technology. Any comments and suggestions will be greatly appreciated.

# Nanomaterial Application Methods

**I**N order to harness the capabilities of nanomaterials it is important to understand how they interact with the environment. Manipulating these patterns of interaction enables us to control the properties that we seek to develop. This chapter focuses on the descriptions of several basic modes of interaction between nanoparticles and the environment we seek to alter. While these topics certainly involve short range transport, a more formal development of transport concepts for nanomaterials will be covered in Section 8.1.

## 1.1. DOPING

Nanomaterials can be built by placing a base material in contact with other materials that are naturally attracted to the base material. For instance, a surface can be immersed in a fluid in which nanoparticles are suspended. The surface may naturally carry a negative charge. If the nanoparticles carry a positive charge, they will be attracted to the surface and stick to it by electrostatic attraction. These positive particles are the dopant in this system. Placing them in contact with the surface to which they will stick is the process of doping. This concept is illustrated in Figure 1.1, where the silica surface carries a negative charge which attracts the positively charged alumina nanoparticles.

The amount of nanoparticles that stick depends upon the size of the nanoparticles and the number of binding sites that occur on the surface. This binding can change the surface energy as well as its charge. The surface in Figure 1.2 can thus be rendered non-attractive toward additional positive particles because it already carries a positive charge.

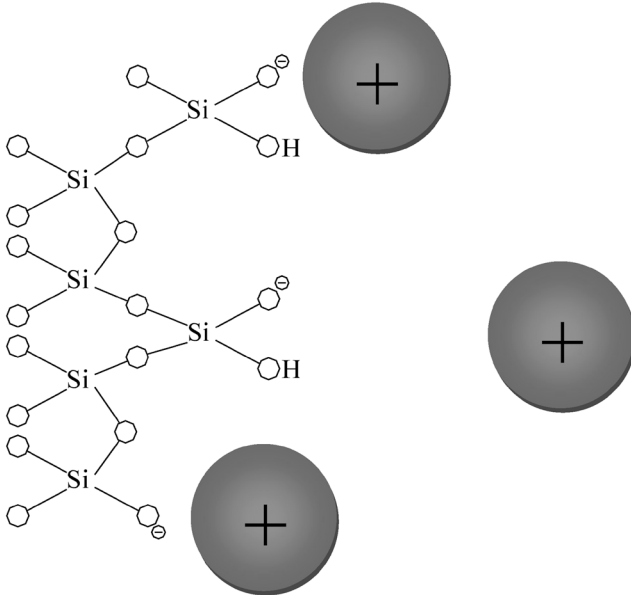


**FIGURE 1.1.** Positively charged alumina nanoparticles electrostatically attracted to a silicate nanostructure immersed in water. The middle-right nanoparticle is repelled from the available bonding site due to electrostatic repulsion from the other two positive particles.

The surface charge of a nanoparticle can also be altered in this manner. In Figure 1.2, a 20 nm particle of silica carrying a negative charge has attracted a number of 2 nm colloidal alumina particles, which have changed the surface charge of the composite particle.

Controlling the surface charge of a nanoparticle is extremely important for controlling transport. The repulsion obtained from a strong surface charge helps minimize the opportunities for particles to collide and stick together. This is referred to as flocking or coagulation. Flocks of particles are less stable in a suspension because gravity has more influence on their motion as they become increasingly massive. At some point, the amount of mass causes gravity to dominate the transport and the particle falls out of suspension.

The sign of the surface charge, positive or negative, will govern the direction of drift. This direction can have a tremendous influence on the outcome of a nanoparticle treatment. For example, if a treatment was designed to drive nanoparticles onto a structure of iron embedded in concrete or soil, a positive surface charge on the particle would mean that the electric field required for treatment would not be expected to hurt the structure. If the particle were negatively charged, then the di-

rection of the electric field would be more difficult to handle. For the example of iron in concrete, the electric field established to drive the particles would cause the iron to dissolve fairly quickly.

The magnitude of the surface charge also influences the velocity of drift that can be obtained when the suspension is subjected to the electric field. The drift velocity that can be achieved per unit of electric field is called electrokinetic mobility. The electric field is simply the voltage potential divided by the distance between the electrodes that are in direct contact with the fluid medium.

## 1.2. ELECTRODEPOSITION COAGULATION ASSEMBLY

When nanoparticles are undergoing electrophoresis they can be driven toward a conductive surface and deposited onto it when they arrive. Since they are repelling each other, the particles tend to space themselves on that surface, occupying places that are not already taken. Thus electrodeposition produces a fairly uniform surface. Figure 1.3 shows large 20 nm particles of silica in the process of losing their covering of 2 nm alumina particles. These smaller particles carry a positive charge and are now able to separate from the silica carrier particle and proceed to the metal surface. The combination of electrostatic attraction to the surface and repulsion from the neighboring particles yields a uniform pattern of electrodeposited spheres. Attraction usually wins the competition, forcing the particles close enough together so that they begin coagulating as a result of van der Waals forces. In general, these forces are

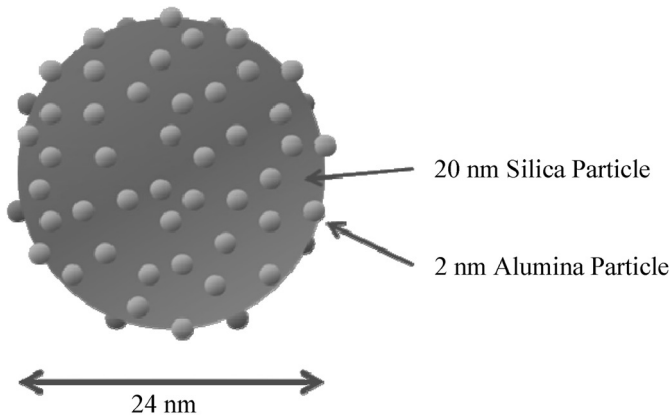


**FIGURE 1.2.** A composite nanoparticle of silica covered with alumina exhibits a positive surface charge. Illustration developed by Dr. Sven Eklund, Louisiana Tech University.

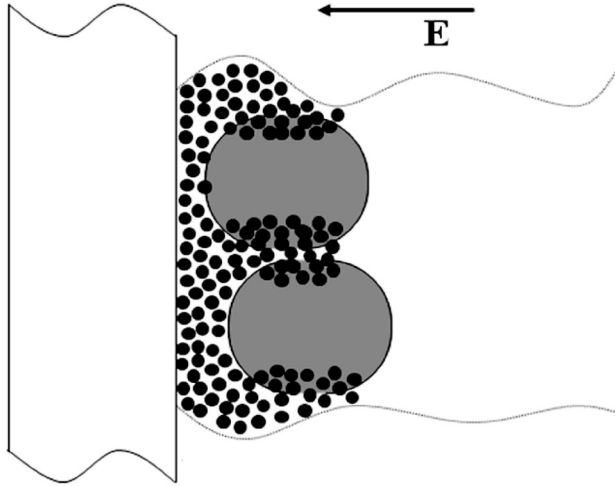


**FIGURE 1.3.** Nanoparticles driven toward an embedded metal flock at the surface, where they form a densely packed electrodeposited phase.

described as weak attractions that exist between molecules. They are at least strong enough to have some influence on the location of a given molecule, atom, or nanoparticle. As in this case they can also manifest between atoms that are located on the surfaces of two nanoparticles that had come into close proximity.

In the case of polymeric particles an additional assembly step is possible. If the system is permitted to dry, polymer chains can uncoil from these particles and begin to interact with neighboring particle

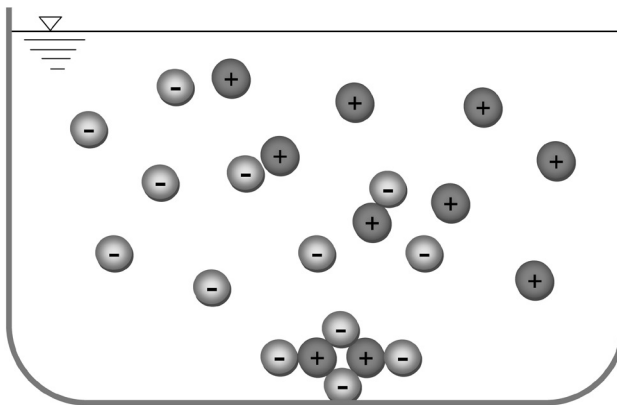


**FIGURE 1.4.** Oppositely charged particles are drawn together via electrostatic attraction. They form electrostatic assemblies that fall out of suspension and drop to the bottom of the beaker.



chains. Over time (hours) this particle assembly can convert itself into a uniform polymer film in much the same way as an organic paint coating.

### 1.3. ELECTROSTATIC ASSEMBLY

If a fluid contains nanoparticles of both positive and negative net charge, they will be attracted and readily stick to each other, just as observed earlier in the description of coagulation. The sticking force in this case tends to be stronger, since it involves both the electrostatic force of the opposing charges as well as the van der Waals forces noted earlier. In Figure 1.4 we see a beaker filled with water. Nanoparticles were added to the beaker, negative ones on the left and positive ones on the right. As the opposing charges draw the particles toward each other, some begin to stick. More particles are added to the coagulated mass until it is too heavy to remain suspended and sinks to the bottom of the beaker (precipitation).

Electrostatic assembly may also involve ions of one charge and particles of the opposite charge. When ions are involved, the opportunity for chemical reaction is significant. Nanoparticles can come under attack. In some cases they may start to dissolve, at which point their own ionic residue becomes available for the formation of new compounds that exhibit ionic or covalent bonding.

### 1.4. SINTERING

This assembly method is typically referred to as powder metallurgy. It is generally conducted in a dry environment in which the particles are subjected to elevated temperature. As shown in Figure 1.5, the contact

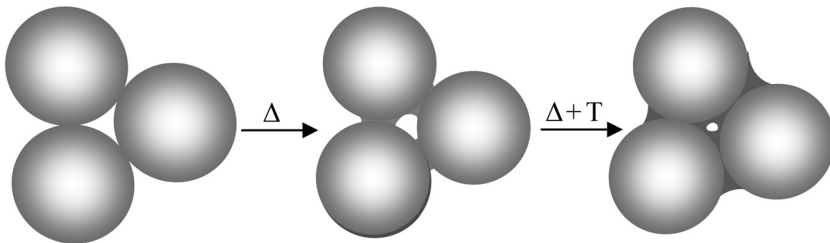


**FIGURE 1.5.** Sintering process starts as temperature is elevated. The higher kinetic energy state of the atoms enables them to diffuse to the points of inter-particle contact. The surface area of the system is reduced during this process, and with it the surface energy.

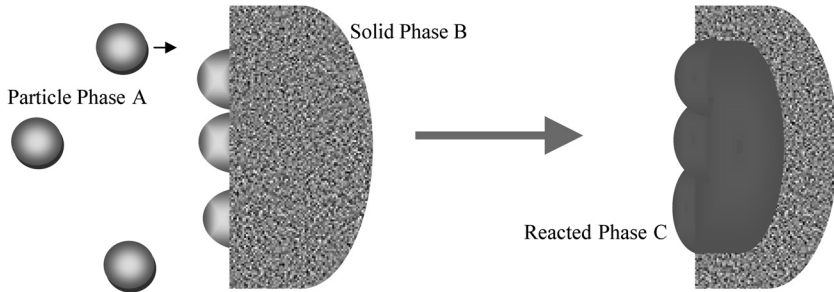


**FIGURE 1.6.** Nanoparticles approach a surface where they adhere and react with the substrate to form a new phase at the surface.

points between the particles are the locations where assembly occurs. Diffusing atoms migrate to these points and form chemical connections to the neighboring particles. The process is driven by the reduction in systemic surface area (and thus in surface energy) that occurs when individual particles are melded together.

## 1.5. REACTIVE CONVERSION

When reactive species of particles arrive at a surface, they can cause a conversion of the surface material to another phase. This process is illustrated in Figure 1.6. A given reaction can be fairly rapid, producing a new phase with distinctive properties. The depth of penetration of this new phase is not expected to be very great. In order for such conversion to occur, the particles must be attracted to the surface by an opposing charge, and then must dissolve at least partially so that ionic derivatives can react with the wall surface. In some cases, the rate of particle transport can be quite short compared with the rate of reaction.

If the reactive surface is along a pore, and the particles are small enough to penetrate it, the reaction may occur deeper within the material. It may occur all along the pore where the reactive wall phase is present. In any location where the pore becomes too narrow to permit particle passage, the penetration will be limited to that point. Other aspects of pore assembly dealing with poor formation are noted in the following section.

## 1.6. PORE ASSEMBLY

All the assembly processes described above can be accomplished

within pores. In some cases the pores can be prepared to make room by modifying the pore system prior to the insertion of nanoparticles or other reactive species. This extension of pore volume can be viewed as a damaging process, since pore formation would take place through micro-cracking and material dissolution. In contrast, the refilling of this additional porosity with new phases that are of greater mechanical strength or chemical resistance can constitute an opportunity for enhanced material performance.

### 1.6.1. Electrochemical Boring

When an electric current passes through a material, the charge transport from a solid to a fluid medium can cause material to dissolve and to be carried through the fluid. In porous material this activity can take place in a pore. This is shown in Figure 1.7. Charges leaving the pore surface will do so as material within the pore is removed. This removal can be localized to phases that are relatively easy to dissolve or to locations in the material that are at a relatively high energy state due to local strain or chemistry. When this material dissolution is so localized, a pore can form or an existing pore can be extended. When it occurs in concrete, the material removed is largely calcium liberated from calcium-bearing phases.

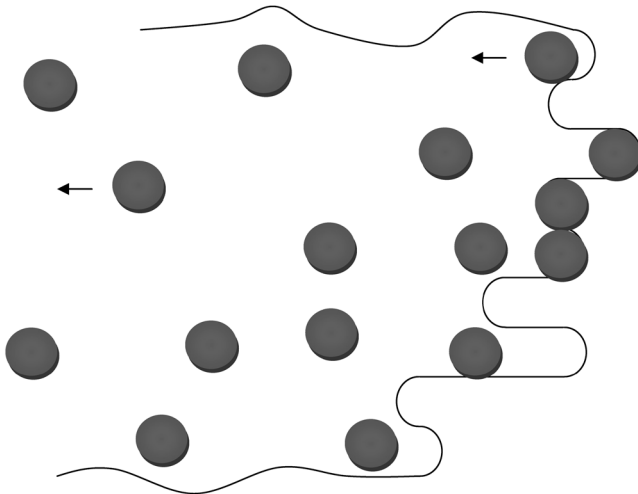


**FIGURE 1.7.** Electrochemical boring extends a pore by causing material within it to jump from the solid state to the ionic state, and to be transported out of the pore.

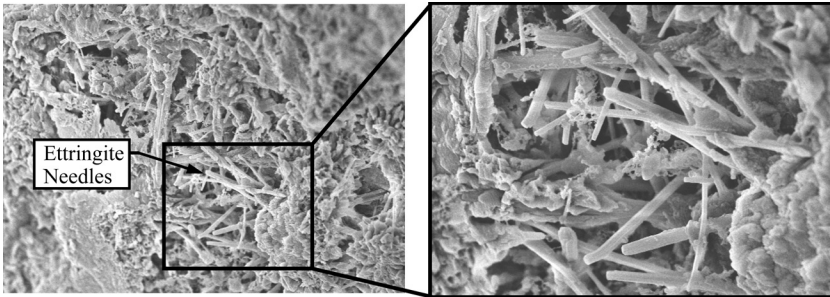


*FIGURE 1.8. The reactive growth of ettringite needles in concrete provides an increase of porosity that is usually unwelcome, but can also provide opportunities for insertion of beneficial species. Image adapted from Kupwade-Patil, K. (2010). Mitigation of chloride and sulfate based corrosion in reinforced concrete via electrokinetic nanoparticle treatment, Ph.D. Thesis, Louisiana Tech University, Ruston, LA.*

### 1.6.2. Reactive Pore Formation

As noted earlier, reactive ionic species can enter the pores of a material and interact with the interior surfaces. This reactivity can produce radical changes to the morphology of the micro/nanostructure. Where new structural geometry is achieved there is the opportunity to increase the porosity of the material. Figure 1.8 contains a scanning electron micrograph of concrete that has been exposed to a solution of calcium sulfate. The sulfates react with the monosulfate phases native to the concrete to produce prismatic needles of ettringite. The growth of these needles open up the pore structure—certainly a damaging occurrence, with an accompanying drop in concrete strength. Examined from another perspective, however, this change presents an opportunity to make room for the transportation of other species into the structure, resulting in a permeating alteration of properties. The pore structure, thus opened, could permit the electrokinetic injection of beneficial species. These may include polymeric particles, or even precursors of them, that could ultimately produce a material exhibiting ductility—which in turn promises better impact or vibration resistance. It could also translate into lower water-permeability and higher strength.

## Electromutagenics

**A**T some point an electrokinetic treatment will cause enough structural and/or chemical change to the microstructure of concrete so that we can consider it a mutated version of the original design. These changes can be described in a hierarchical order. The lowest order is simple reduction in porosity. Next is the conversion of chemical phases achieved by an introduced agent. Then comes the development of entirely new phases obtained exclusively from introduced species. These changes can happen side by side with any changes occurring to the existing phases. The following sections describe examples of how such changes are achieved.

### 9.1. PORE STRUCTURE REVISION

When nanoparticles fill a pore without reacting with any other species, they can form a densely packed structure within the pore. The new porosity consists of interparticle spacing. The remaining porosity is located in pores that did not receive particles, as well as in locations at pore walls that are too small for an additional particle, but larger than the interparticle spacing.

In Figure 9.1 the results of mercury intrusion porosimetry tests are shown for several specimens of concrete, each with a 0.5 w/c content (Kupwade-Patil, 2010). The highest curve in this collection pertains to a control sample that did not receive a particle treatment. The curve shows that the pores ranged from 0.05 to 1000 microns. In addition, 25% of the pores were less than 10 microns. Next consider the case in

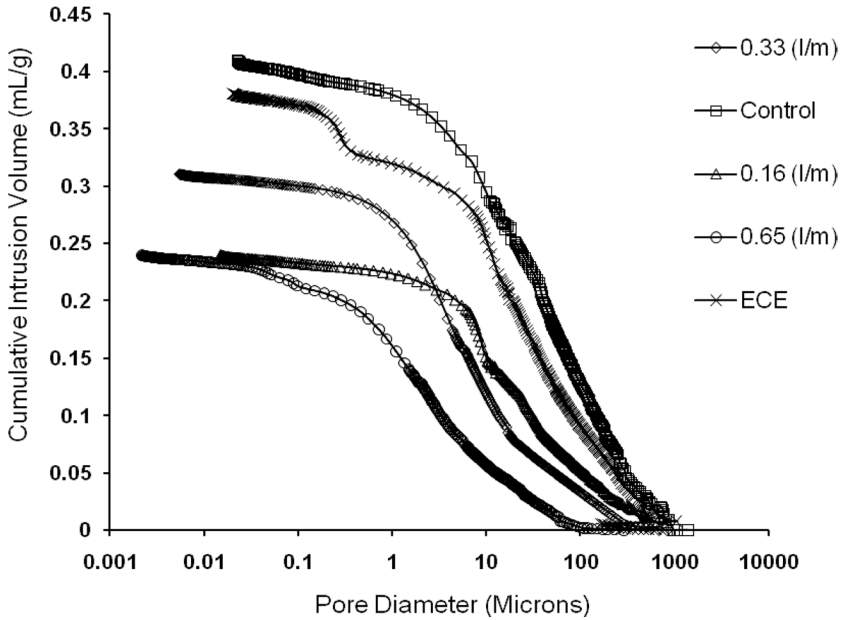


FIGURE 9.1. Mercury induced porosimetry (MIP) curves on powdered concrete two inches away from the concrete. Adapted from Kupwade-Patil, 2010 with permission.

which electrokinetic treatment was conducted with a 24 nm silica particle with a dosage of 0.65 l/m<sup>2</sup> of concrete surface. The total volume of pores in a gram sample dropped from 0.41 to 0.24 ml. The pore sizes ranged from 2 nm to 100 microns. Of these pores, 75% are less than 10 microns. The electrokinetic treatment clearly reduced the pore volume of the material. The sizes of the pores observed were also smaller.

Figure 7.2 illustrates the elimination of microcracks in limestone (Cardenas, *et al.*, 2007). Cracking was induced by 12 cycles of freezing and thawing at temperatures ranging from 0–70° F daily for 12 days. Cracking causes an increase in porosity. Cracks like the one observed in Figure 7.2 were no longer encountered after a treatment of calcium ions and sodium silicate. After treatment, the material was also relatively free of the extremely fine-grain detail.

The shrinkage and/or elimination of pores constitutes the simplest level of electromutagenic processing. In this case, the process was a little more complex, since it involved the introduction of a new phase (C–S–H) (Cardenas *et al.* 2007). It was achieved throughout a 5-inch wall section. The treatment was conducted using a vertically-oriented sponge electrode.

The porosity reduction in this case was approximately 40%. The change in strength associated with this case was 82%.

## 9.2. CHEMICAL ACTIVATION/MICROSTRUCTURAL PHASE REVISION

In this class of mutation, the electric field injects a species that reacts with phases present inside the solid matrix of the concrete. The new phase created may add to the quantity already present, or introduce a species that is closely related to those native to the system. The following sections describe how such transformations can be achieved.

### 9.2.1. Calcium Hydroxide Conversion

When silica and alumina nanoparticles are driven into pores of concrete, an opportunity arises for the conversion of calcium hydroxide into C–S–H and C–A–H phases. These are the pozzolanic reactions associated with silica fume, fly ash, and other sources of silica and alumina.

The fundamental pozzolanic reaction is the hydration of silica or alumina. In the presence of calcium hydroxide, these reactions may be expressed as follows:  $\text{CH} + \text{S} + \text{H} \rightarrow \text{C} - \text{S} - \text{H}$  (calcium silicate hydrate), as well as the alumina analogue,  $\text{CH} + \text{A} + \text{H} \rightarrow \text{C} - \text{A} - \text{H}$  (calcium aluminate hydrate), (Mindess *et al.* 2003, p. 42).

Initially,  $\text{OH}^-$  ions attack the O–Si or O–Al bonds of the mineral. As more of these bonds are broken, ions of silica or alumina enter solution, and the hydroxyl ions attach themselves to silicon or aluminum atoms. Silicate and aluminate anions develop and form an amorphous material balanced by  $\text{H}^+$ ,  $\text{K}^+$ , and  $\text{Na}^+$  ions from the capillary pore fluid. Later, available  $\text{Ca}^{+2}$  reacts with the amorphous material to form the final C–S–H or C–A–H type products. These reactions often proceed much more slowly and with lower heat evolution than is exhibited by the primary hydration reactions of Portland cement (Taylor, 1997, p. 280). Reactivity of flyash is also dependent on the structure of the individual particles. Flyashes with dense glassy surface layers can require pre-treatment with basic solutions in order to corrode surface layers and make interior sites accessible for enhanced reactivity (Fan *et al.*, 1999). In the case of silica fume, densified forms exhibit slower reaction rates, presumably due to the reduction in available bonding sites (Sanchez de Rojas, 1999).

Several variants of calcium aluminates have been observed in or-



dinary Portland cement as well as high alumina cements (Taylor, p. 298, 1990). Calcium aluminate can form chemically unstable phases,  $C_2AH_8$  and  $CAH_{10}$ ; and both of phases can transform to  $C_3AH_6$ . This new phase is higher in density than either of the others. This causes an increase in porosity. The use of alumina-coated silica nanoparticles causes a small amount of  $C_2AH_8$  formation (Figure 9.2). It has the classic hexagonal crystal habit of such unstable phases. The new phase is cubic and significantly denser.

It is interesting to note that concretes found to exhibit  $C_2AH_8$  retained higher strength than untreated companion specimens. Probably this is due to the alumina portion of a given nanoparticle constituting only 2% of the total particle mass, the rest being silica. Also, the insertion of particles causes porosity to drop and strength to increase even when the reaction is not taking place. In one case it was observed that only 8% of the calcium hydroxide in the concrete had been converted to C-A-H or C-S-H. Clearly the rest of the nanoparticles were not able to access the remaining calcium hydroxide in the concrete. The hardened cement paste phase can easily contain as much as 50% or more calcium hydroxide. Strength gain of the nanoparticle-treated concrete was probably influenced by  $C_2AH_8$  only to a small extent. This means that the conversion  $C_3AH_6$  is more than matched by the other strength-enhancing influences of the treatment.

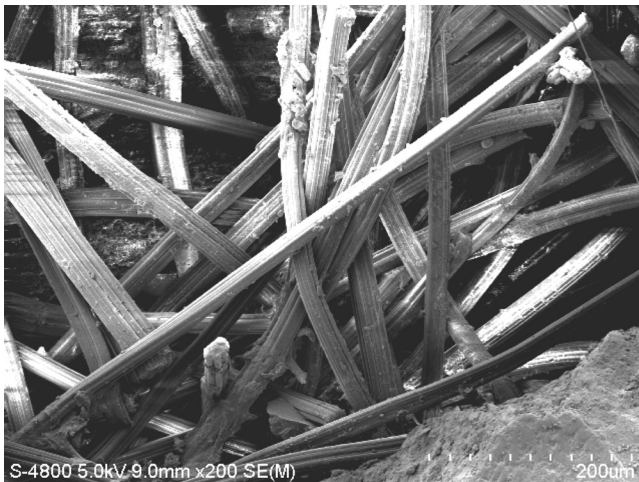
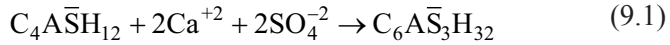


**FIGURE 9.2.** Magnified image showing striated needles of di-calcium aluminate hydrate ( $C_2AH_8$ ). Reproduced from Kupwade-Patil et al. June 2011 with permission from ASCE.



### 9.2.2. Monosulfate Conversion

Sulfates entering cement capillary pores come into contact with monosulfate. These species react to form ettringite as follows:



At some stage, gypsum may also form. Gypsum does not contribute to matrix destruction until sulfate content exceeds 1000 mg/l (Mindess *et al.* 2003, p. 487). Solid volume expansions due to the formation of gypsum and ettringite are reported at factors of 2.2 and 2.8 respectively (Zivica, 2000).

Long prismatic needles of ettringite as well as gypsum have long been believed to be the source of expansion leading to disruption of the cement matrix (Solberg and Hansen, 2001). More recent work has examined the role of C–S–H decalcification. This loss of calcium in the binder matrix has come to be recognized as a major source of strength reduction that could account for a good deal of concrete structure degradation (Taylor, 1997, p. 373). In other work (Odler and Colan-Subauste, 1999), a significant portion of expansion is associated with water imbibitions. Ettringite crystals of colloidal dimensions have been found to take up significant amounts of water osmotically, leading to expansion and damage (Mehta and Wang, 1982).

Differences in the severity of sulfate attack have been observed that depend on the counter ion. Especially severe degradative influence has been exhibited by  $MgSO_4$  (Bonen, 1994; and Rasheeduzzafar *et al.*, 1994). It has been suggested that the  $Mg^{2+}$  participates in the degradation process. When  $Mg^{2+}$  is present, brucite and  $M_3S_2H_2$  precipitates have been observed in addition to ettringite (Gollop and Taylor, 1992). Ettringite formation utilizes calcium, leading to decalcification of C–S–H.

Calcium carbonate has been found to contribute carbonate ions that substitute for sulfate ions in ettringite and monosulfate structures (Kakali *et al.*, 2000). Due to the relatively low solubility and high stability of calcium carbonate, it was found that a partial substitution of calcium carbonate for ordinary Portland cement delayed the transition of ettringite to monosulfate.

As shown in Figure 9.3, ettringite needle formation causes a significant change in microstructure when monosulfate is converted. The new microstructure is clearly more porous. When the sulfate ions are

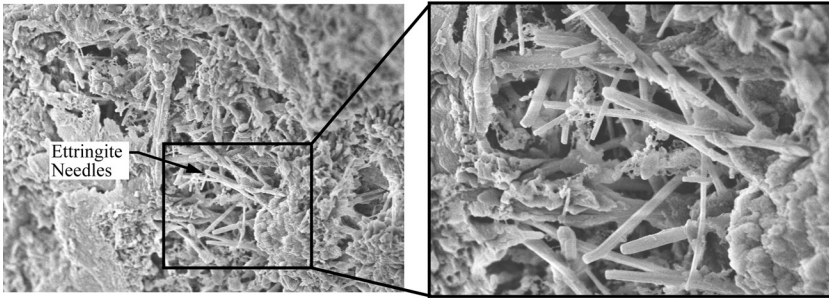


**FIGURE 9.3.** The action of sulfates increases pore sizes in concrete, creating opportunities to inject species that provide other benefits such as anti-biological agents. Adapted from Kunal Kupwade-Patil, 2010 with permission.

removed from the concrete, the degradation slows down. Once the existing ettringite needles have been saturated with absorbed water, the damage due to expansion can be expected to stop.

Because the microstructure now contains larger pores and microcracks that can be considered an extension of porosity, the opportunity exists for injecting other species into this altered pore structure—for example, loading the expanded pores with biocide particles such as copper oxide or a titanium dioxide. Since pore modification due to sulfate attack left the concrete in a weaker state, other nanoparticles of silica can be incorporated in order to recover strength.

This may seem outlandish, but it is conceivable that the intentional injection of sulfates could be accomplished in a calculated attempt to increase porosity temporarily. The altered pore structure could then be loaded with other beneficial species. Afterward, or even during the final stage of treatment, the sulfate ions still left in the pore fluid could be extracted by reversing the circuit polarity that was used to inject them.

### 9.3. POLYMERIC PHASE ASSEMBLY

The development of polymer-enhanced concrete has involved the use of dehydration, saturation with polymer precursors, and the application of gamma radiation to trigger polymerization. The results were impressive in terms of strength and durability; but lacked practicality. The following section describes an electrokinetic approach that can be used to avoid the use of dehydration and gamma radiation.

The key here is to find a polymer precursor somewhat soluble in water and carrying a net charge when dissolved. Methyl methacrylate

(MMA) is one such species. It is the precursor for poly methyl methacrylate (PMMA). A key feature of this monomer is that it can be induced to polymerize in the presence of a basic pH.

Figure 9.4 illustrates a treatment process involving MMA (Nayeem and Cardenas, 2011). The monomer is slightly soluble in water. It carries a negative charge that permits the use of electrokinetic transport into the pore structure. Driving this species directly to the reinforcement presents an interesting opportunity. The monomers at a very low dilution of say 1–2% will have relatively little opportunity to make contact with each other while in transit to the reinforcement. This reduces the chances of premature polymerization that could effectively limit a significant amount of monomer from loading.

Once a monomer arrives at the reinforcement, it must wait for another monomer to arrive before the elevated pH of the pore fluid can trigger a polymerization reaction. Similarly, this newly polymerized pair will wait for the next arrival before polymerization continues. In this way, the polymerization process can start at the reinforcement and continue growing fibers of polymer back through the pore.

In a preliminary PMMA synthesis trial conducted with the assistance of James Eastwood at the applied electrokinetics laboratory at Louisiana Tech University in September of 2008 the current density combined with the specimen geometry led to the curious extrusion of fibers from the top of the specimen (Figure 9.5). These submicron fibers grew in less than a week of treatment using an extremely high current density of  $5 \text{ A/m}^2$ .

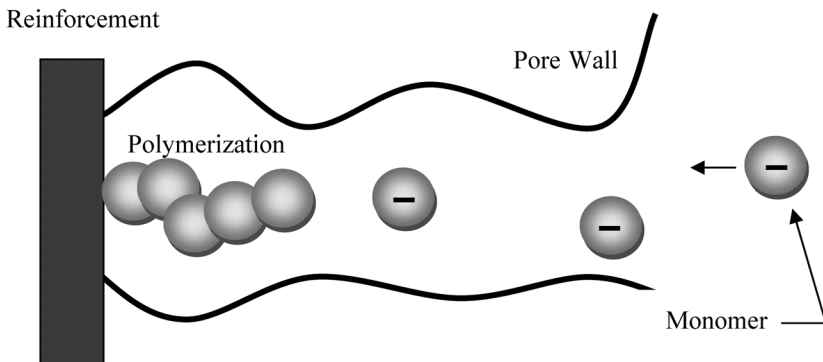


**FIGURE 9.4.** Methyl methacrylate is slightly soluble in water and carries a negative net charge. When it is drawn to the reinforcement, the elevated pH of the concrete pore fluid causes it to polymerize.

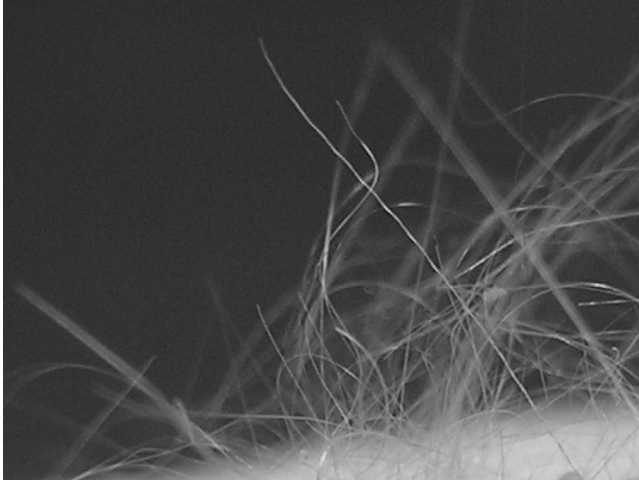


*FIGURE 9.5. Fibers of PMMA ranging from 10–100 microns extruded from the surface of a specimen of hardened cement paste during an electrokinetic treatment.*

Another trial conducted with a reduced current density of  $1 \text{ A/m}^2$  and a treatment time of 12 days resulted in no extrusion of fibers (Nayeem and Cardenas, 2012). The tensile strength of the hardened cement paste increased 50% from 950 psi to 1500 psi. Figure 9.6 shows a fracture surface in which a fiber can be seen protruding from a pore.

The implications of synthesizing and growing polymers within the pores of concrete are interesting. Whisker formation of most materials tends to cause unusually high strength to develop, because the defect concentration in a whisker of material is often lower than that achieved in a bulk process. In the current case, the opportunities for defects to exist in the cement pores is quite low, due to the isolated and protected nature of the environment. In fact the electric field drawing methyl methacrylate toward the interior of the specimen is also drawing most ions out of solution and toward either pole of the circuit. This can clearly increase the purity of the processing environment. A similar analysis to that conducted in Section 7.4 was used to estimate the tensile strength of the PMMA phase formed in this case. The preliminary estimate indicated a tensile strength of 19 ksi for these whiskers, 80% higher than is typical for PMMA. While this increase in strength may seem surprising, it is certainly consistent with the differences in strength observed when whiskers of materials are compared with bulk strength (Stepanov, 1995; and Berezhkova, G., 1973). Material whiskers, being relatively

low in defects, have been shown to exhibit tensile strengths that are a factor of 2–10 higher than the bulk material.

The other interesting implication of this concept has to do with corrosion protection. The first line of defense is typically a surface coating. Since no such coating is defect free, it is a matter of time before aggressive species such as chlorides get past a surface barrier that is typically less than 0.005 in thickness. A PMMA formation would require minimal to no surface preparation, and would provide a barrier coating that ranges 2 inches from the reinforcement to the concrete surface. As this barrier forms, it also displaces the water out of the pore system, starting at the rebar interface and working outward. The solvated PMMA ions can almost certainly penetrate some of the smallest (1–2 nm) pores of hardened cement paste. This level of pore saturation would have a dramatically suppressive impact on corrosion processes at the reinforcement.

A couple of interesting dilemmas confront the prospect of forming PMMA at the concrete reinforcement. One concern is the polarity required to drive negative ions to the reinforcement—a polarity that will cause the iron reinforcement to corrode. The second concern is the need for an elevated pH to trigger the polymerization process. Older concrete loses high pH due to the natural processes of carbonization and leaching.

A re-alkalizing pre-treatment of the steel reinforcement can remedy

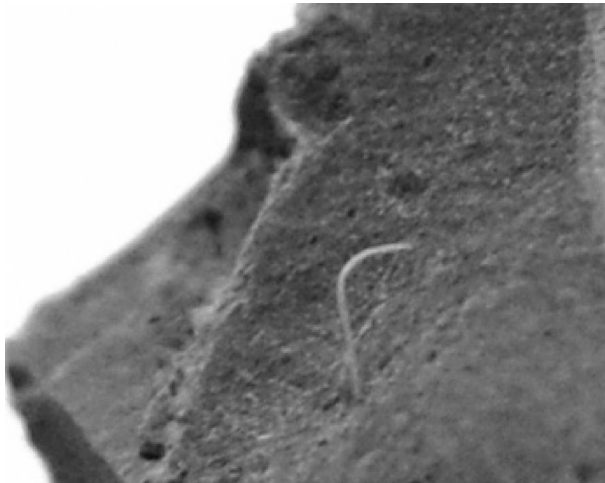


*FIGURE 9.6. Single fiber of PMMA emanating from a pore on a fracture surface of a hardened cement paste specimen.*

both concerns. Re-alkalizing concrete involves electrokinetic treatments using calcium, sodium, and potassium hydroxides, in which various oxides of these metals are electrodeposited on the surface of the reinforcement. It was noted earlier that a combination of all 3 hydroxides can be used to form a sacrificial coating on iron reinforcement, while the polarity needed to drive MMA into the concrete removes it. Re-alkalization also resolves the pH concern, because the formation of the ceramic protective layer causes the pH in the vicinity of the reinforcement to rise substantially. This condition thus provides the pH needed for the precursors to polymerize as they reach the reinforcement.

#### **9.4. NANOCOMPOSITE PHASE ASSEMBLY**

This approach is based in part on the principal of electrostatic layer-by-layer assembly achieved by alternate adsorption of oppositely-charged nanoparticles and/or ions. In this case, the process is actually more electrodynamic in nature because weak electric fields are used to transport the charged species into the pores of the cementitious material. Various combinations of treatments were conducted over a period of 7 to 14 days. The following sections describe how these treatments were carried out and the interesting characteristics that they produced in concrete masonry blocks.

##### **9.4.1. Combining Modes of Assembly**

Layer-by-layer (LbL) self-assembly by alternate adsorption of oppositely-charged components (polyelectrolytes, nanoparticles and proteins) was developed in 1998 as a simple and versatile nanotechnology for thin coating surfaces (Lvov, Decher and Möhwald, 1993; Ichinose, Lvov and Kunitake, 2003; and Decher, 1997). These assemblies are usually in the vicinity of 10–500 nm. In related work, LbL assembly was conducted within 500 nm alumina pores for template synthesis of nanotubes (Li and Cui, 2006). No attempt had been made to apply this nanoassembly method to ordinary Portland cement until 2007.

In traditional LbL assembly, sequential adsorption of oppositely-charged components is carried out on a solid surface, such as a glass slide. The substrate is alternately immersed solutions or suspensions of polycations and negative nanoparticles. This mode of assembly is now combined with electrokinetic transport in order to create a reaction zone within the pores of concrete. In some cases, different species known to

# Index

- adsorption, 100
- alumino-silica, 10
- assembly
  - coagulation, 3
  - electrodeposition, 3
  - electrostatic, 5
  - layer-by-layer, 158
  - polymeric, 4
  - pore, 6
  - reactive, 6–7
- basement seepage, 10
- beam treatment setup, 57–58
- boring electrochemical, 7
- bottlenecking, 30
- bridge deck, 134, 159–160
  - particle treatment design, 142–145
  - treatment setup, 134
- C–A–H phase creation, 68
- calcium aluminate, 83, 152
  - phases, 68
- calcium carbonate, 68, 87, 153
- calcium hydroxide, 68
  - conversion, 68, 151–152
- capillary
  - draw, 129
  - drying, 128
  - forces, 105
  - wetting, 105
- carrier fluid, 89
- cathodic protection, 134
- cement, 9
  - double layer, 111
- cement paste nanostructure, 110–111
- cement pore fluid, 111
- ceramic coating for rebar, 138–142
- charge alumina, 1
- charge double layer, 107–112
- charge particle, 108
- charge silica, 1
- chemical activation, 151
- chloride
  - extraction, 33, 56
  - limits, 61
  - sources, 56
- chlorine gas generation, 128
- circuit
  - charge carriers, 130
  - polarization, 129
- coagulation, 2, 30
- coating limitations, 88
- coefficient
  - coupling, 100
  - electroosmotic permeability, 112–114
- cold joints, 41
- colloid stability, 11
- column treatment setup, 135

- composite, 93
- concrete
  - young, 128
- concrete pH, 55
- conduction
  - ionic, 11, 106
- conductivity, 99, 104–106
  - coefficients, 99
  - electrical, 100
- consolidated phase strength, 94
- contaminants, 55
- corrosion
  - costs, 56
  - chloride, 55
  - current density, 59
  - damage, 55
  - iron in concrete, 55
  - linear polarization, 59
  - measurement, 55
  - pH and, 55
  - rate of, 59
  - rebar, 55
    - severity of in, 60–61
    - resistance, 55
- crack(s), 10, 83, 94
  - crack repair, 10, 41, 42
  - micro, 83
  - pores, 84
- cracking, 73
  - limestone, 90
  - sulfate, 76
  - tensile, 56
- C–S–H, 9
  - decalcification, 111
  - double-layer, 111
  - formation, 93
  - nanosstructure, 110
  - pH, 110
  - phase creation, 67
  - pore wall, 111
  - tobermorite, 110
- damage recovery, 30, 96
- damage repair, 87
- damage recovery, 96
- Darcy's Law, 11, 103–104, 113
- decontamination, 56, 83
- dielectric constant, 107
- diffusion, 100–104
  - coefficient, 101
  - gas, 103
  - liquid, 103
  - vapor, 103
- dopant, 1
- doping, 1
- double layer, 112
- drag force, 111
- ECE, 33, 56
  - effectiveness, 56
- electric field, 3, 30, 106, 115
  - distribution, 132
  - lines, 132
- electric current
  - damage, 57
  - reduction, 129
- electric circuit polarization, 129–130
- electric current
  - drop, 130–132
  - limit, 135
- electric potential drop, 132
- electrical
  - conductivity, 100
  - connection design, 134
  - contact, 129
  - double layer, 109–112
  - potential, 100
  - resistance, 25
- electrochemical boring, 7
- electrochemical chloride extraction, 56
- electrode
  - configuration, 30
  - electrode corrosion protection, 138–142
  - crack repair, 47
  - degradation, 133
  - design, 135–136
  - distribution, 30
  - packing treatment, 31
  - packing, 32
  - particle packing, 46
  - placement, 47–50
  - design, 133



- electrode (*continued*)
  - polarization, 130
  - shape, 132
  - stress concentration, 50
- electrodeposition, 3
  - alkali metal, 138–142
- electrokinetic
  - process design, 99
  - transport, 105
  - treatment design, 99
- electrokinetics
  - electroosmosis, 105
  - electrophoresis, 105
  - ionic conduction, 105
- electromutagenics, 149
  - phase revision, 151
  - pore structure revision, 149–150
  - processing, 166
- electroosmosis, 10–11, 17, 100, 108, 109–111, 114
  - direction, 112
  - measurement cell, 13
  - small-large pore theory, 112
  - solution impact, 112
- electroosmotic
  - coefficient, 114
  - flow, 111–112
  - velocity, 109–114
  - volume flow rate, 112
- electrophoresis, 3, 11, 107
- electrophoretic mobility, 16, 114, 120
  - transport control volume, 116
  - velocity, 114
  - volume flow, 125
    - rate, 117
- electrostatic charge, 1
  - coagulation, 163
  - particle, 1
- electrosynthesis, 154–158
- ettringite, 73, 80, 83, 153–154
  
- flocculation, 117
- flocking, 2
- floor treatment setup, 136–137
- flow, 99–100
  - continuity, 103
  - coupled, 100
- flow (*continued*)
  - electroosmotic, 111–112
  - electrophoretic volume, 117
  - hydraulic, 100–103
  - laminar, 103
  - plug, 109–110
  - volume, 103–104
    - rate, 116
- fluid
  - carrier, 89
  - penetration, 105
- fly ash, 12
- force
  - electrophoretic retardation, 106–107
  - relaxation, 106–107
  - viscous drag, 106, 108–111
- formation factor, 104
- foundation treatment setup, 136–137
- freeze-thaw damage, 87–88
  - damage mechanics, 95
- FTIR, 68–83
  
- gas
  - barriers, 128
  - formation, 128
- gel space ratio, 49
- gradient pressure, 115
- gradients, 99
  - chemical, 99
  - electrical, 99
  - hydraulic, 104
  - potential, 100
  - pressure, 99
  - thermal, 99
- grout, 10
- gypsum, 80, 153–154
  
- healing microcracks, 87
- hydraulic “coefficient, permeability”, 11
- hydrogen gas generation, 128
  
- ion, 105
  - cloud, 106
  - conduction, 105
  - drift, 106
  - transport forces, 106

- layer-by-layer assembly, 158
- limestone, 87
  - composite, 93
  - macrocracks, 83
  - water movement, 88
- masonry, 88, 158
  - block, 37–38
  - porosity reduction, 163
  - water movement, 88
- mass transfer, 101
- mercury intrusion, 30
- microcracks, 12, 83
  - healing, 87
  - micropores, 94
  - repair, 95
- micropores,
  - microcracks, 94
- microstructure revision, 151
- MIP, 34, 59, 63, 105
  - limitations, 105
  - sulfate damage, 78
- modulus
  - prediction, 50
  - rupture, 43
- monosulfate conversion, 83, 153
- nanocomposite
  - assembly, 158
    - phases, 158
  - chloride barrier, 61
  - concrete penetration, 113
  - corrosion barrier, 57, 61
  - high-current compensation, 121
  - mobility, 120
  - phase creation, 66–67
  - pozzolanic, 57
  - process design, 99
- Ohms law, 100
- Onsager reciprocity principle, 109
- particle(s)
  - charge, 24
  - coagulation, 2, 21
  - composite, 2
  - corrosion barrier, 57
- particle(s) (*continued*)
  - dosage, 33
  - electrophoresis, 3
  - film assembly, 164
  - flocculation, 117
  - mass action, 33
  - mobility, 16–17
  - packing, 122
    - density, 31–34
    - efficiency, 118
  - penetration in concrete, 115
    - model, 115–119
  - pile-up, 31
  - polymeric, 4
  - self-assembly, 163
  - size ratios, 45
  - transport, 11, 30
    - control volume, 115, 122
    - inhibition, 128–129
    - model, 120
    - rate, 120
    - particle reactivity, 21
    - time calculation, 143–144
  - treatment
    - design, 122
    - effectiveness, 130–131
    - surface impacts, 124
    - voltage, 121
- patch interface, 41–43
- permeability, 9–26, 104
  - coefficient, 104
  - hydraulic, 103
  - impact, 131
- pH,
  - C–S–H, 110
- phase
  - conversion, 149–151
  - creation,
    - C–A–H, 67
    - C–S–H, 68
  - consolidated, 93
  - expansion, 153–154
  - polymer, 154–158
  - strength, 156
- plombierite, 24
  - X-ray diffraction, 23
- plug flow, 110

- PMMA, 154
- polymer
  - precursor, 154
  - reaction, 154–158
  - self-assembly, 154–155
  - whiskers, 156–157
- pore(s)
  - capillary, 11
    - absorption, 103
    - forces, 105
  - connectivity, 12, 35, 104
  - diameter, 62
  - drying, 128
  - fluid in cement, 111
  - modification, 154
  - packing simulation, 45
  - percolation limit, 15
  - re-wetting, 129
  - size impact, 121
  - sizes in concrete, 121
  - surface absorption, 103
  - tortuosity, 35
  - wall
    - charges, 111
    - nanostucture, 111
- porosimetry, 30, 59, 63, 105
  - limitations, 105
- porosity, 9, 113–114
  - drying impact, 128
  - masonry block, 163
  - MIP, 30
  - modeling, 48
  - reduction, 9, 29–30, 45, 52, 80, 149
    - limit, 46
    - values, 121–122
  - strength, 48–49
- powder metallurgy, 5
- pozzolan, 10–11
- pozzolan
  - reaction, 12, 21, 151
  - products, 69
  - sulfate effect, 12, 74
- Raman spectroscopy, 66, 81, 82
- reactive treatment, 21, 23
- re-alkalization, 157–158
- rebar
  - corrosion, 55
  - electrode corrosion protection, 138–142
  - protection layer, 33
  - treatment, 33
- reciprocity principle, 109
- resistance change, 25
- resistivity
  - change, 25
  - ratio, 25–26
- shrinkage, 128
- silica, 166
  - fume, 10
  - particles, 89
- slag, 12
- sodium silicate, 89
- spallation sulfate attack, 76
- sponge electrode, 58, 88–89, 123–126, 135
- stone, 87
  - water movement, 88
- streaming, 109
  - current, 109
  - potential, 109
- strength
  - masonry block, 38, 161–162
  - nanoparticle compensation, 121
  - prediction, 50
  - recovery, 74
  - reduction, 77, 153
    - factor, 44
- sulfate, 12
  - attack, 30, 73–77
  - decontamination, 83
  - extraction setup, 137–138
- surface,
  - “area specific”, 104
  - energy, 103
  - tension, 105
  - wetting, 105
- tobermorite, 110
- tortuosity, 122
- transport, 11, 99–105
  - drivers, 99

- gradients, 99
- in concrete, 100
- treatment
  - beams, 33
  - bridge deck, 134
  - corrosion, 129
  - design, 136, 142–145
    - parameters, 122
  - effectiveness, 25, 37
  - masonry block, 37, 159–160
  - preventative, 96
- tri-calcium aluminate, 74
- van der Waals, 3–4
- velocity
  - ion drift, 106–107
  - electroosmotic, 109–111
  - electrophoretic, 108
- vertical surface treatment, 88
- volume flow, 116
- wall treatment setup, 135
- X-ray diffraction, 69
- zeta potential, 108, 111–112

## About the Author

**H**ENRY E. CARDENAS, PH.D. is the Jack T. Painter endowed Professor of Civil Engineering at Louisiana Tech University, Ruston. He is also Associate Professor in the Departments of Mechanical as well as Nanosystems Engineering. Connecting the dots across a range of disciplines has brought Dr. Cardenas international recognition for his award winning research in which nanomaterials are being applied to a variety of practical problems. He is the director of the Applied Electrokinetics Laboratory in the College of Engineering and Science. With over 25 years of experience in Defense, industrial and academic research, he has over 40 publications in the area of materials performance and durability.